Influence of different carbon nanotubes on the mechanical properties of polyaniline nanocomposite – multiscale molecular modeling

M. IONITA[a*], V. CIUPINA[b], E. VASILE[c]
[a]*University Politehnica of Bucharest, Bucharest, 060042, Romania*
[b]*Ovidius University of Constanța,Constanta, 900527, Romania*
[c]*Metav-CD, Bucharest, 020011, Romania*

In this work we present a computational routine based on molecular mechanics, dynamics and dissipative particle dynamics to predict mechanical properties and morphology of polyaniline (PANI), PANI-single walled carbon nanotubes octadecylamine (SWCNTs-ODA) functionalized and PANI-SWCNTs carboxylic acid (SWCNTs-CA) functionalized composite systems. Computational models of PANI-SWCNTs-ODA and PANI-SWCNTs-CA were implemented at atomistic and meso-scale. Computational results clearly confirmed that SWCNTs-ODA and SWCNTs-CA are properly dispersed and have beneficial effect on PANI mechanical properties. The Young's moduli generally increased with increasing SWCNTs content and values range from 2.77 GPa in the case of pure PANI to 7.39-9.31 GPa in the case of PANI-SWCNTs-PABS composite system.

(Recieved July 14, 2011; accepted July 25, 2011)

Keywords: Multiscale molecular modelling, Polyaniline, Single walled carbon nanotubes, Mechanical properties

1. Introduction

Polyaniline (PANI), is one of the most promising polyconjugated polymers, distinguished by good conducting properties, stability, and a relatively easy production process; furthermore, its raw materials are available and inexpensive [1-2]. However, PANI films present wick mechanical properties which are relevant for most of its applications [2]. The combination of carbon nanotubes (CNTs) with conducting polymers offers an attractive route to reinforce polymer as well as to introduce electronic properties based on morphological modification or electronic interaction between the two components [3-5]. The development of such nanocomposites which can bring in the CNTs excellent properties is one of the hottest research areas of the moment. The construction of superior nano structured composite depends on the dispersion of carbon nanotube in the polymer matrix or homogeneity of the material which was reported to be dependent of CNTs nature [4-8]. In the case of single walled carbon nanotubes their insolubility and poor compatibility with the polymer make the uniform dispersion in the polymer matrix very difficult, and the resulting inhomogeneous nanocomposites often have unsatisfying properties [7-8]. Instead the use of carbon nanotubes chemically functionalized, attached by covalent bonds to the polymer matrix seems to be a good approach for synthesizing homogeneous polymer/carbon nanotubes composites [4, 9-10]. It has been demonstrated that by simply combing the polymer with the suitable carbon nanotubes and by choosing the relative weight ratio carbon nanotubes/polymer the features of the resulting material can be finely tuned [10]. However, this it will results in high number of materials and compositions which is costly and time consuming to test with experimental techniques. Computer-aided molecular modeling can be a valid tool to reduce the material characterization efforts moreover allows the evaluation of the dependency of the properties on the material composition [4, 12-13]. It has been shown recently that atomistic level simulations using the MD technique can successfully compute the mechanical properties of a variety of polymers and polymer/carbon nantubes composites [12–14] although there are very few works reporting the computational characterization of polymer/CNTs composites since performing these simulations is not a trivial task. It can be difficult to obtain mechanical properties from atomistic simulation that compare well with experimentally measured values due to the difficulty of building the models and the various parameters involved [14]. Recently we have reported atomistic simulations of PANI/single walled carbon nanotube (SWCNTs) composite systems but this first foray was not successful due to approximation of some features of the real material [14]. Our previous experience in this area has led us to adopt a policy of ensuring that the computational models represents as accurately as possible the real network, relying on experimental data such as, polymer tacticity, density of the real material, number of repeated units within the polymer chains *etc*. On the other hand the prediction of the CNTs dispersion and alignment within polymer matrices would allow for the rational decisional process for the definition of new and improved nanocomposite materials. Computational molecular

modeling at mesoscale has been demonstrated to accurately reproduce material morphology [15-17]. Dissipative Particle Dynamics (DPD) is one of most known mesoscale simulation approach; it is based on a bead-spring-bead approach, introduced in an attempt to go beyond the limitations of atomistic MD simulations, whilst retaining some molecular details including the hydrodynamic interactions [15-17].

In this work, a routine for generating feasible atomistic models of PANI-SWCNTs chemically functionalized with different groups (carboxylic acid (CA) and octadecylamine (ODA)) composite materials and calculating the elastic constants is described. Further atomistic simulations were used to derive solubility parameters values among all system components (PANI, SWCNTs-ODA and SWCNTs-CA), which were further used to calculate mesoscale simulation parameters and mesoscale simulations were performed to determine composite systems morphologies.

2. Materials and methods

2.1 Realization of atomistic bulk models

The models of the repeating units of the polymeric chains (aniline), CA and ODA groups were manually constructed and then minimized in order to obtain a stable starting structure. Charge groups have been assigned to fragments of each repeated unit and all structures were properly equilibrated employing a standard algorithm, starting with a steepest-descent stage, switching to conjugate gradient when energy derivative reaches 100 kcal·mol^{-1}Å^{-1} followed by Newton-Raphson optimization algorithm. The final convergence criterion was to meet a derivative of less than 0.001 kcal·mol^{-1}Å^{-1}. The polymeric chains were then generated starting from the repeating units using the "Build Polymers" tool of the software. Carbon nanotube (5, 6) is available as standard model in Materials Studio data base. Further SWCNTs-ODA and SWCNTs-CA structures were implemented by constructing a covalent bond between SWCNTs (5, 6) and ODA or CA groups. Using the structures previously created and equilibrated for each of the materials, PANI, PANI-SWCNTs-ODA and PANI-SWCNTs-CA, independent atomistic bulk models were generated employing "Amorphous Cell" tool of Materials Studio with 95/5 and 91/9 (w/w) ratios, employing the Amorphous Builder. The main characteristics of the bulk models are depicted in Table 1. The bulk models were grown at 300K under cubic periodic boundary conditions using the COMPASS forcefield [18]. Since the systems contain aromatic elements the chain packing stage was performed for all the models at a very low initial packing density (typically 0.1 g/cm3) as Hofmann and co-workers [19] suggested.

2.2 Refinement of atomistic bulk models

All initial packing models were subject to an extensive multistage equilibration procedure composed of a sequences of energy minimisation, NPT (constant number of molecules, pressure and temperature) and NVT (constant number of molecules, volume and temperature) ensembles – MD simulations as reported in Table 2. First the models were slowly compressed from a density of about 0.1 g/cm^3 to the respective real density via NPT-MD runs at p = 1 GPa and T = 300 K for about 5000-7500 steps. After the compression stage the systems present a certain degree of unrealistic tension this indicates that the simulated packing models need to be equilibrated. Equilibration was performed by running a minimization step of 300 ps and a series of NVT-MD simulations at 750K, 600K, 450K, and 300K each one for 300 ps. The equilibration routine was repeated until computational bulk model reach the density of the real material [19-20].

Table 1. Bulk model main features.

Model	Composition of the model [w/w]	Model density [g/cm^3]	No. of atoms in the model	Av. lateral dimension of the model (Å)
PANI	100	1.23	7204	41.84
PANI/SWCNTs-ODA	95/5	1.29	7644	41.93
PANI/SWCNTs-ODA	91/9	1.32	8084	42.92
PANI/SWCNTs-CA	95/5	1.29	7548	42.11
PANI/SWCNTs-CA	91/9	1.33	8084	42.04

From Ref. [29] the density of PANI is 1.23 g/cm^3 and the density of SWCNTs is 1.4 g/cm^3.

Table 2. Stages of equilibration routine.

Stage of equilibration	Ensemble	Temperature (K)	Time (ps)
1	Minimisation	0	300
2	NPT-MD	300	5-7
3	Minimisation	0	300
4	NVT-MD	750	200
5	NVT-MD	600	200
6	NVT-MD	450	200
7	NVT-MD	300	300

2.3 Characterization of the atomistic models

The computational bulk models mechanical properties and isotropy were evaluated testing the mechanical behaviour of the models in three orthogonal directions using the Mechanical Properties Assessment tool implemented in the software. Elastic Properties Analysis tool is using a static approach originating in the work of Theodoru *et al*., 1986 in more details described elsewhere [21].

2.4 Realization of mesoscale bulk models

Amorphous Cell analysis module was further employed to predict solubility parameters δ of composite system components using the Scatchard and Hildebrand theoretical treatments of mixing [22-23]. Afterwards Flory Huggins theory and dissipative particle dynamics mesoscale molecular modeling was used to estimate the SWCNTs-ODA and SWCNTs-CA dispersability within PANI matrices.

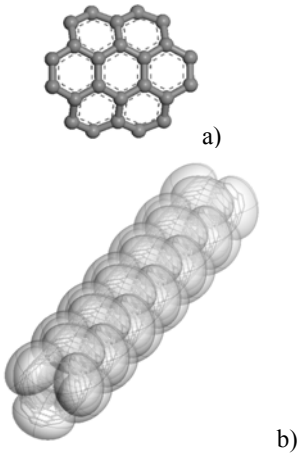

Fig. 1. Coarse graining atoms to beads for SWCNTs model, representation of one bead of SWCNTs a) and SWCNTs mesoscale model b).

DPD simulations for PANI-SWCNTs-ODA and PANI-SWCNTs-CA were conducted using DPD module of Materials Studio software. In present study each PANI monomer, aniline, is represented with a single bead. The PANI chains considered in present study consisted of 100 beads. For SWCNTs mesoscale models six aromatic rings (Fig. 1a) were represented with a bead and each SWCNTs consisted of 24 beads as depicted in Fig.1b. Computational cubic bulk models of PANI-SWCNTs-ODA and PANI-SWCNTs-CA were implemented with different compositions 91/9, 95/5 (w/w) within a simulations box of 20×20×20 reduced units (r.u.) consisting of 2.4 *10000 beads. The beads of the same molecule are connected by harmonic spring having the spring constant c = 4. The DPD calculations run over $2*10^5$ steps with a time step of 0.05 reduced units. As Groot and Warren suggested density of the system was set ρ=3 r.u. [24].

3. Results and discussion

The present simulation routine combine atomistic and mesoscale simulations and was focused to generate and characterize computational systems with large SWCNT-ODA and SWCNTs-CA weight fraction (5% and 9%). Although experimental system typically contain much lower weight fraction of CNTs, our simulations results can help to make useful prediction for lower CNTs weight fraction enhancement by extrapolation. The equilibration routine allows the obtainment of suitable computational bulk models, energetically stable which reflect well the density of the real material. In Figure 2, is depicted the characteristic computational bulk model of PANI-SWCNTs-ODA (95/5 w/w) which consists of about 8000 atoms and two components.

3.1 Mechanical properties assessment

A first investigation of the computational bulk models was performed by evaluating the models' Young modulus and isotropy by means of virtual uniaxial traction tests along their three perpendicular edges. The method used here for calculating the elastic constants is a method for static deformation of periodic atomistic models. The 6×6 elastic constant matrix is determined by partial derivatives of the stress tensor σ, with respect to the deformation, ε, as indicated by equivalent-continuum constitutive equation

(1). The constitutive equation of the equivalent continuum is given as follows:

$$\sigma_{ij} = C_{ijkl}\varepsilon_{kl} \quad (1)$$

Where, σ_{ij} are the components of stress tensor and C_{ijkl} is the elastic constant matrix [17]. By reversing elastic constant matrix, the compliance matrix (2) was obtained and the elastic moduli referred to the three perpendicular direction of the cell.

$$\begin{matrix} 1/E_1 & -\nu_{21}E_2 & -\nu_{31}/E_2 & 0 & 0 & 0 \\ -\nu_{12}/E_1 & 1/E_2 & -\nu_{32}/E_3 & 0 & 0 & 0 \\ -\nu_{13}/E_1 & -\nu_{23}/E_2 & 1/E_3 & 0 & 0 & 0 \\ 0 & 0 & 0 & 1/\mu_{12} & 0 & 0 \\ 0 & 0 & 0 & 0 & 1/\mu_{13} & 0 \\ 0 & 0 & 0 & 0 & 0 & 1/\mu_{14} \end{matrix} \quad (2)$$

where, E is Young's modulus, μ is shear modulus and ν is Poisson ratio. The stiffness (3) and inverse compliance matrix (4) for PANI-SWCNTs-CA (91:9 w/w) is reported below.

$$\begin{matrix} 8.559 & 3.946 & 4.369 & 0.381 & 1.414 & -0.163 \\ 3.996 & 11.81 & 3.826 & 0.524 & -0.176 & -0.233 \\ 3.818 & 3.905 & 15.11 & 0.543 & 1.082 & -0.867 \\ 0.495 & 0.443 & 0.340 & 3.858 & 0.075 & 0.413 \\ 1.173 & -0.139 & 1.293 & 0.039 & 2.609 & 0.148 \\ -0.265 & -0.086 & -0.668 & 0.378 & 0.1608 & 3.545 \end{matrix} \quad (3)$$

$$\begin{matrix} 0.161 & -0.045 & -0.028 & -0.005 & -0.0790 & 0.001 \\ -0.047 & 0.106 & -0.016 & -0.007 & 0.0401 & 0.000 \\ -0.022 & -0.018 & 0.080 & -0.008 & -0.0232 & 0.019 \\ -0.013 & -0.004 & -0.002 & 0.264 & 0.0023 & -0.032 \\ -0.064 & 0.035 & -0.028 & 0.003 & 0.4341 & -0.026 \\ 0.011 & -0.005 & 0.014 & -0.030 & -0.0293 & 0.290 \end{matrix} \quad (4)$$

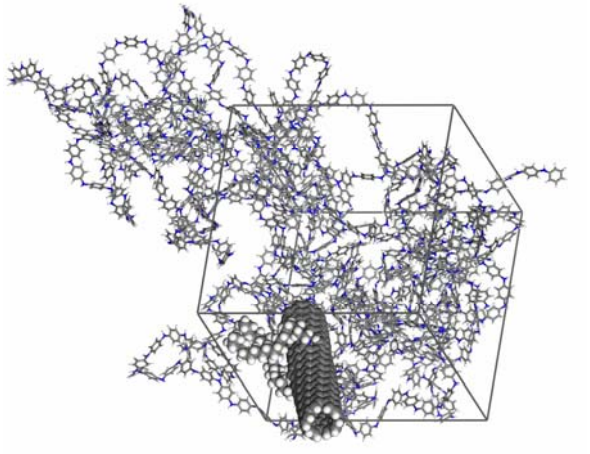

Fig 2. Packing model for PANI-SWCNTs-ODA 95:5 (w/w). SWCNTs-ODA is emphasised for better visualisation.

The results of virtual traction tests are summarized in Table 3. These values are taken from the average of the three configuration runs for a given set of parameter values. The results of the mechanical properties assays showed that for each one of the composite materials, the values of the Young modulus along the three perpendicular directions were very disagreeing; this is indicating that the computational systems characteristic to PANI-SWCNTs-ODA and PANI-SWCNTs-CA are not isotropic. For what concern the numerical values we expect to see an increase of Young's moduli values for increasing CNTs content. Generally, this trend is observed with some inconsistencies which are discussed below. The predicted Young's moduli from the MD simulations at 300 K range from 2.77 GPa in the case of pure PANI, to 4.74-5.72 GPa in the case of PANI-CNTs-ODA, and 7.39-9.31 GPa in the case of PANI-SWCNTs-CA composite materials. An increase of up to 300% of the elastic moduli was observed upon the addition of approximately 9 wt. % SWCNTs-CA.

The reinforcement was related on the one hand to the systems composition and on the other hand to the systems components. As displayed in Fig 3 higher values of CNTs percentage cause an increase of materials stiffness, this effect becomes evident for CNTs fraction of about 5 wt%. Doubling the CNTs content (from 5 wt. % to 9 wt. %) the values of Young's modulus increase has not the same extent. This suggests that the optimum CNTs reinforcement is perhaps below 9 wt%. Similar trend for elastic constants was found in the work of Zeng at al. [25]. They observed an increase of the elastic constants of poly(methyl methacrylate) as the carbon nanotubes content increase up to 5 wt%, for higher content of carbon nanotubes just marginal effect was observed. On the other hand, the Young's moduli were related to the material components as depicted in Fig. 3. Generally, there is an increase of Young's modulus with the addition of CNTs, the maximal value of Young's modulus (9.31 GPa) was obtained for the composite system PANI-SWCNTs-CA (91/9 w/w) thus we can conclude that the best reinforcement of PANI is provided by SWCNTs-CA.

Table 3. Young's moduli on three perpendicular directions of PANI, PANI-SWCNTs-ODA and PANI-SWCNTs-CA computational systems with different compositions obtained by means of molecular modeling

	Model composition (w/w)	Ex (GPa)	Ey (GPa)	Ez (GPa)	Eavg (GPa)
PANI	100/0	2.96	2.13	3.22	2.77
PANI-SWCNTs-ODA	95/5	4.98	3.57	5.68	4.74
PANI-SWCNTs-ODA	91/9	3.96	6.38	6.82	5.72
PANI-SWCNTs-CA	95/5	7.52	6.11	8.54	7.39
PANI-SWCNTs-CA	91/9	6.17	9.36	12.40	9.31

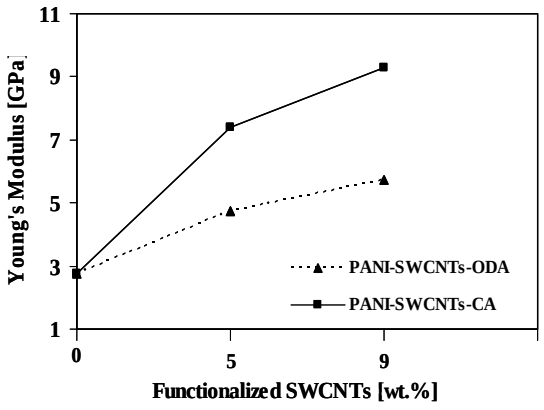

Fig. 3. Young's modulus trend as a function of SWCNTs-CA and SWCNTs-ODA content.

The differences in the reinforcing efficiency between SWCNTs-CA and SWCNTs-ODA is mostly likely due to different interaction energies/interfacial adhesion between the carbon nanotubes and PANI. Interfacial adhesion quality was estimated assuming Flory-Huggins theory on the base of solubility parameters [26]. Flory-Huggins theory predicts that components with similar δ values lead to small repulsions, accordingly PANI (δ=20.89(J/cm^3)$^{-0.5}$) should present a the best interfacial adhesion with SWCNTs-CA (δ=23 (J/cm^3)$^{-0.5}$) and good interfacial adhesion with SWCNTs-ODA (δ=26 (J/cm^3)$^{-0.5}$). The predicted Young's modulus values from MD simulations of PANI and PANI composite systems are in good agreement with theoretical and experimental results from the literature which range from 2-4 GPa for PANI and are up to 17 GPa for the PANI-CNTs composites [3, 27-28]. In these reports we can notice that the mechanical properties of the resultant PANI material and its composites might changed due to the characteristics of PANI material such as molecular weight, doping or the preparation of films or fibers [3]. Conversely, small discrepancy might appear between experimental and computational values due to the fact that in the present models some features of the real material such as the presence of voids and imperfections were not taken into account.

3.2 Models morphology assessment

In order to analyze the SWCNTs-CA and SWCNTs-ODA dispersion within PANI matrix DPD mesoscale simulation technique was employed. DPD provides a dynamics algorithm with hydrodynamics for studying coarse-grained systems over long length and time scales. In DPD calculations a small region of material (group of atoms) is represented by a single bead, therefore the number of particles to be simulated is reduced with the respect to atomistic simulations. The beads mutually interact via soft potentials. Three forces are acting between each pair of nonbonded beads: a conservative force, F_{ij}^{C}, interaction which is linear in the bead-bead separation; a dissipative force, F_{ij}^{D}, representing the viscous drag between moving beads, and a random force, F_{ij}^{R}, representing stochastic impulse. The nonbonded interactions between a pair of nonbonded beads can be written as:

$$f_i = \sum_{i \neq j} \left(F_{ij}^{C} + F_{ij}^{D} + F_{ij}^{R} \right) \tag{5}$$

Groot and Warren [24] established a link between this conservative force and the Flory-Huggins interaction parameter, χ, which is a measure of the compatibility of binary mixtures. Flory-Huggins interaction parameter could be calculated from solubility parameters (atomistic simulations) [26].

$$\chi_{ij} = \frac{\left(\delta_i - \delta_j\right)^2 V}{RT} \tag{6}$$

where, δ_i and δ_j, are the solubility parameters of i and j, respectively, while V is the molar volume of the bead, R is universal gas constant, and T is temperature. Subsequently, Flory-Huggins parameters were converted into repulsion parameters (a_{ij}) between pairs of beads using equation (7) [17].

$$a_{ij} = \frac{\chi}{0.306} + 25 \tag{7}$$

In addition, there is also a harmonic force between bonded beads. Bonded beads interact by Hookean springs controlling the bond stretching and angles bending. A single spring constant is used to specify the average bonded interaction. All forces are short-ranged with a fixed cut-off radius, r_c, set as unit length.

Table 5. Van Krevelen solubility parameters and molar volume of composite systems components.

System component	Van Krevelen Parameter ((J/cm^3))$^{-0.5}$	Molar Volume (cm^3/mol)
PANI	20.89	75.53
SWCNT	26	110
CA	23	89.44
ODA	26	43.02

Fig. 4 illustrates the morphology of PANI-SWCNTs-CA and PANI-SWCNTs-ODA composite systems after 2*10 ^{5} DPD calculation steps. In Fig. 4a, 4b it can be easily observed that SWCNTs-CA and SWCNTs-ODA are well embedded into the PANI matrix and singularly dispersed regardless of their concentration. Therefore, the improvement of mechanical properties observed by means of atomistic molecular modeling is reasonable and in good agreement with our DPD observations and data from the

literature [3-4, 25]. Interestingly, similar trend for Young modulus was found in the work of Gajendran *et al*. [3] and Gojny *et al*. [30-31].

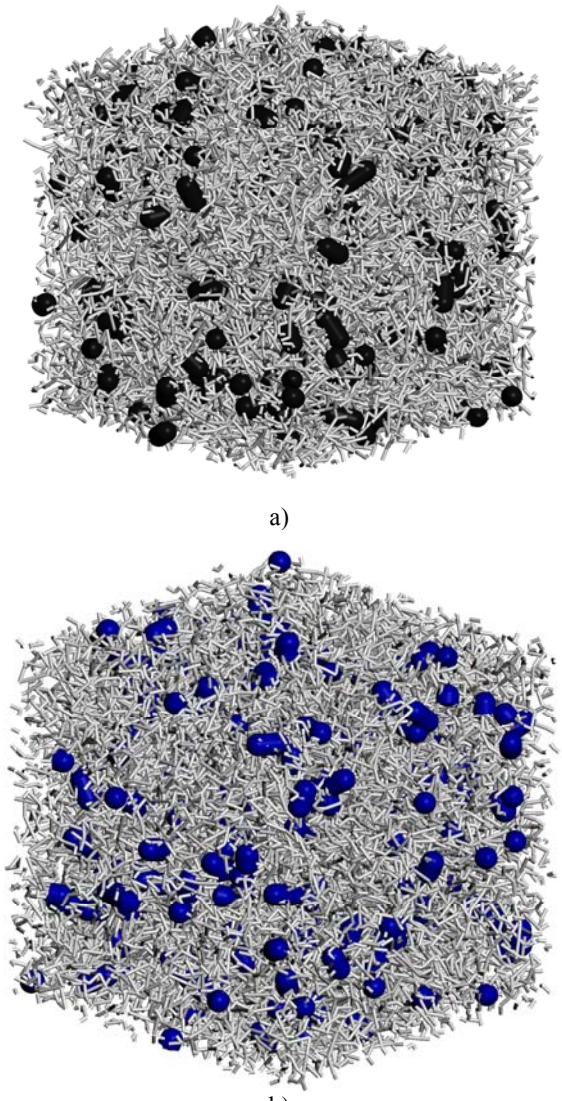

a)

b)

Fig. 4. Equilibrium morphology of PANI-SWCNTs-CA (91/9 w/w) a) and PANI-SWCNTs-ODA (91/9 w/w) b) systems as modelled by DPD. SWCNTs-CA are shown in black, SWCNT-ODA are shown in dark blue and PANI chains are shown in light grey.

They observed an increase of the Young modulus, when the CNTs are well dispersed within polymer matrix, on the opposite when CNTs are agglomerated a decrease of polymer Young's modulus was observed.

4. Conclusion

This work confirms that MD and DPD computational tools allow to achieve well equilibrated bulk models and to predict PANI, PANI-SWCNT-ODA and PANI-SWCNTs-CA composite systems properties accurately.

The simulation results suggested the possibility of mechanically reinforce PANI by incorporation of SWCNTs-CA or SWCNTs-ODA. Among the studied composite systems PANI-SWCNTs-CA exhibited the highest enhancement of the Young's modulus and it was followed by composites PANI-SWCNTs-ODA.

The reinforcement of PANI was found to be a function of SWCNTs content: while at 5 wt% CNTs loading, the modulus of the composite systems increased substantially, similar improvements were not observed at 9 wt% CNTs loading. This suggests that the optimum CNTs reinforcement is perhaps below 9 wt%.

The results of simulations agree with theoretical considerations, which forecast higher Young's moduli with higher CNTs content.

DPD simulations suggested that both SWCNTs-CA and SWCNTs-ODA are properly dispersed within the PANI matrix.

Acknowledgements

This research has been supported by the National Research Grant PN-II-RU-TE-_153, CNCS-UEFISCDI**.**

References

[1] T. A. Skotheim, R. L. Elsenbaumer, J. R. Reynolds (Ed.). Handbook of Conducting Polymers, 2nd ed., Marcel Dekker, New York (1998).
[2] P. Chandrasekhar. Conducting Polymers, Fundamentals and Applications: A Practical Approach, Kluwer Academic, Boston (1999).
[3] P. Gajendran, R. Saraswathi, Pure Appl. Chem. **80**, (2008).
[4] M. Ionita¸ I. V. Branzoi , L. Pilan, Surf. and Interface Anal. **42**, (2010).
[5] S. J. Park, S. Y. Park, M. S. Cho, H. J. Choi, M. S. John, Synth. Met. **152**, (2005).
[6] M. Wong, M Paramsothy, X. J. Xu, Y. Ren, S. Li, K. Liao, Polymer **44**, (2003).
[7] J. Gou, B. Minaie, B. Wang, Z. Liang, C. Zhang, Comp. Mater. Sci. **31**, (2004).
[8] E.T. Thostenson, T.W. Chou, J. Phys. D: Appl. Phys. **35**, (2002).
[9] H.Tan, L.Y. Jiang, Y. Huang, B. Liu B, K.C. Hwang, Compos. Sci**.** Technol.**67**, (2007).
[10] D.Guo, H. Li, J. Solid State Electrochem. **9**, (2005).
[11] L.Y. Jiang, Y. Huang, H. Jiang, G. Ravichandran, H.Gao, K.G. Hwang, J. Mech. Phys. Solids, **54**, (2006).
[12] Y. Han, J. Elliott, Comput. Mat. Scie. **39**, (2007).
[13] A. Gautieri, M. Ionita, D. Silvestri , E. Votta, S. Vesentini, G.B. Fiore, N. Barbani, G. Ciardelli, A. Redaelli, J. Comput. Theor. Nanosci. **7**, (2010).
[14] T.C. Clancy, S.J.V. Frankland, J.A. Hinkley, T.S. Gates, Polymer **50**, (2009).
[15] A. Maiti, J. Wescott, P. Kung, G. Goldbeck, Int. J. Nanotech. **2**, (2005).
[16] A. Maiti, J.Wescott, P. Kung, Mol. Sim. **31**, (2005).

[17] Materials Studio 5.0 software (Accelerys, Inc. UK) tutorial.
[18] H. Sun H. J. Phys. Chem. B. **102**, (1998).
[19] D. Hofmann, L.Fritz, C. Ulbrich, C. Schepeers, M. Bohning, Macromol. Theory Simul. **9**, (2000).
[20] E. Tocci, D. Hofman, D. Paul, N. Russo, E. Drioli, Polymer **42**, (2001).
[21] D.N. Theodorou, U.W. Suter, Macromolecules **18**, (1985).
[22] S.G. Scatchard, Chem. Rev. **8,** (1931).
[23] J.H. Hildebrand, J. Am. Chem. Soc. **38**, (1916).
[24] R.D. Groot, P.B.Warren, J. Chem. Phys. **107**, (1997).
[25] J.Zeng, B. Saltysiak, W.S Johnson, D.A. Schiraldi, S. Kumar, Composites: Part B: Eng. **35** (2004).
[26] P.E. Rouse, J. Chem. Phys. **21**, (1953).
[27] V. Mottaghitalab, G. M. Spinks, G. G. Wallace, Synth. Met. **152**, (2005).
[28] V. Mottaghitalab, B. Xi, G. M. Spinks, G. G. Wallace, Synth. Met. **156**, (2006).
[29] J. Stejskal, M. Trchova, N.V. Blinova, E.N. Konyushenko, S. Reynaud, J. Prokes, Polymer. **49**, (2008).
[30] F.H. Gojny, M.H.G. Wichmann, B. Fiedler, K. Schulte. Comp. Scie. Technol. **62**, (2005).
[31] F.H. Gojny, M.H.G. Wichmann, U. Kopke, B. Fiedler, K. Schulte. Comp. Scie. Technol. **64**, (2004).

*Corresponding author: mariana.ionita@polimi.it